Ultra-short, Beamed Source of Laser-driven Epithermal Neutrons

S. R. Mirfayzi,[1,2] T. Mori,[2] D. Rusby,[3] C. Armstrong,[3] H. Ahmed,[1] M. Borghesi,[1] C.M. Brenner,[3] R.J. Clarke,[3] Z. E. Davidson,[4] D. Doria,[5] C. P. Jones,[6] P. McKenna,[4] D. Neely,[3] T. B. Scott,[6] A. Yogo,[2] and S. Kar[1,3,*]

[1] *Centre for Plasma Physics, School of Mathematics and Physics, Queen's University Belfast, BT7 1NN, UK*
[2] *Institute of Laser Engineering, Osaka University, Suita, Osaka, 565-0871, Japan*
[3] *Central Laser Facility, Rutherford Appleton Laboratory, Didcot, Oxfordshire, OX11 0QX, UK*
[4] *Department of Physics, SUPA, University of Strathclyde, Glasgow, G4 0NG, UK*
[5] *Extreme Light Infrastructure - Nuclear Physics, IFIN-HH, 077125 Magurele, Romania*
[6] *Interface Analysis Centre, Wills Physics Laboratory, Tyndall Ave, Bristol BS8 1TL, UK*

(Dated: March 7, 2019)

Development of intense neutron sources driven by laser will enable a range of scientific investigations and new opportunities for industrial and medical applications. In particular, an ultra-short, point-like source of epithermal neutrons using laser-driven ultra-short ion pulses would open new opportunities for many unprecedented time-resolved spectroscopic and imaging applications. This paper reports the first measurement of the ultra-short bursts of epithermal (sub-MeV) neutron beams using intense lasers, produced predominately by the endothermic ^{7}Li(p,n)^{7}Be reaction at the near energy threshold. Using a ^{6}LiF scintillator in time-of-flight arrangement, epithermal neutrons of $\sim 10^{7}$ n/sr/pulse in the range of 20-200 keV were measured, which intrinsically offers a beamed feature and ultra-short duration. The mechanism of epithermal neutron production and the cross-calibration of the diagnostic employed for extending the spectral measurements down to epithermal range are discussed.

PACS numbers: Valid PACS appear here

Recent progress in laser-driven sources has enabled the production of sub-ns neutron pulses useful for many applications in science [1], industry [2, 3], security [4] and healthcare [5] either directly, or by moderating [6] down to thermal and epithermal ranges. The laser-driven neutron sources, in particular, the light ions driven beam-fusion reactions, are of high interest due to their brightness, directionality, and compactness[7]. While the laser-driven ions produce an ultra-short (sub-ns), point-like (few mm wide) source of fast neutrons, to produce lower energy neutrons e.g. epithermal, moderation is used. This is typically a highly inefficient process, and destroys the unique features, such as the small source size and ultra-short burst duration, of the fast neutron source. On the other hand, if it makes it possible to generate epithermal neutrons directly from a target bombarded by the laser-driven ions, it will open an entirely new territory of frontier applications exploiting its unprecedented ultra-short (sub-ns) duration and small (mm) source size, such as time-resolved resonance spectroscopy[8], flash imaging in a point projection configuration with high spatial resolutions.

As of today, the production of short bursts of epithermal neutrons is currently limited to large-scale facilities, such as ISIS spallation source. Instruments such as Very Low Angle Detector (VLAD) at VESUVIO spectrometer [9] at ISIS are designed to perform High Energy Inelastic Neutron Scattering (HINS) measurements, [10] on an inverse geometry time-of-flight (tof) scheme to extend the kinematic region currently investigated by neutron scattering experiment. A shorter pulse length would therefore leads to higher energy resolution, or, for a given energy resolution, will allow reducing the source to detector distance leading to a higher flux of transported neutrons at the sample location.

Among the possible light-ion driven nuclear reactions, the endothermic ^{7}Li(p,n)^{7}Be reaction can produce neutrons of sub-MeV energies when triggered by protons of energy close to its reaction threshold (~2 MeV). Energies in this range can be efficiently produced using lasers, for instance via Target Normal Sheath Acceleration (TNSA) [11]. Using protons produced from conventional accelerators, this particular reaction is currently used for studying neutron-induced activation of rare isotopes[12], as well as in nucleosynthesis [13] of heavy elements to study astrophysical phenomena via different capture processes. Using laser-driven ions, on the other hand, would allow producing the epithermal neutrons with burst durations that have never been produced before.

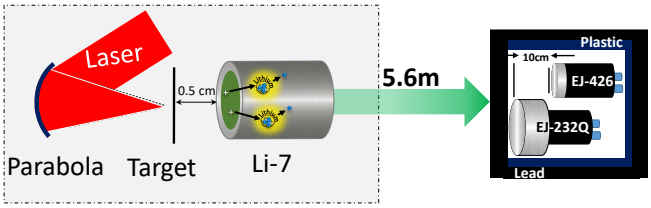

FIG. 1. Schematic of the experimental setup, showing the pitcher-catcher mechanism in producing neutrons via ^{7}Li(p,n)^{7}Be reaction, diagnosed by EJ-426 and EJ232Q scintillators.

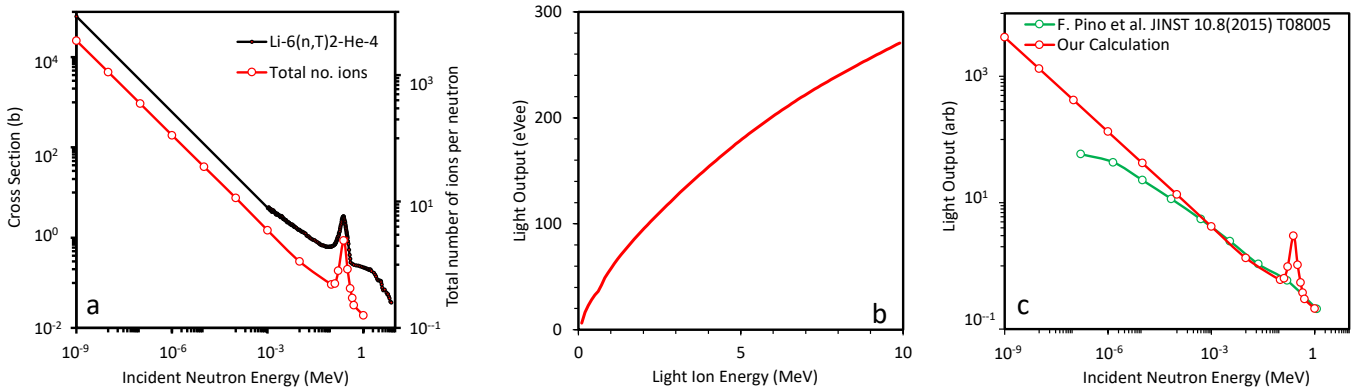

FIG. 2. **a)** The black line shows the capture cross section given for $^6Li(n,T)^2He$ reaction. The red line shows the number of alpha particles created by neutrons of different energies, obtained by irradiating 1 μm thick EJ426 scintillating medium, using FLUKA simulations. **b)** The corresponding light output calculated in units of equivalent-electron energy from Chou's semi-empirical formulae reported in Refs [15, 22] from the EJ426 scintillator when irradiated by alpha particles of different energies. **c)** Shows the relative weighted average light output from the detector compared with the data from literature [23].

Using the laser-driven accelerated protons in a pitcher-catcher configuration [14], production of epithermal neutrons from the ^{7}Li(p,n)^{7}Be reaction was studied on a proof-of-principle basis. The epithermal neutrons produced from the near-threshold reaction were diagnosed by time-of-flight (ToF) technique using a ^{6}LiF scintillator sensitive to low energy neutrons. Cross-calibrating the data obtained from this detector with a previously calibrated fast neutron scintillator [15], an epithermal flux of $\sim 10^7$ was measured at the source in the range 20-200 keV. Monte-Carlo simulations were carried out to corroborate the part of the measured spectra corresponding to the fast neutrons, while the epithermal part of the spectrum matches to that obtained by other groups from the near-threshold reaction using conventional accelerator beams. Although the angular distribution of the epithermal neutrons was not measured in the experiment, the evaluated nuclear database, as reported in Ref [16] suggests a strong anisotropic emission of the epithermal neutrons, compared to the emission profile of the fast neutrons, those produced by the higher energy protons.

The experiment was carried out using the VULCAN laser of the Rutherford Appleton Laboratory (RAL), UK [17]. The ~1.5 ps FWHM laser pulse with the energy ~30 J was focused on 10 μm thick Au target by a f/3 off-axis parabola, delivering peak intensity of $\sim 5\times 10^{19}$ Wcm^{-2} on the target. Energetic protons up to ~10 MeV were produced mainly via the TNSA mechanism. The protons were used to generate neutrons by impinging on a 1 cm thick block of ^{7}Li converter (henceforth called the catcher) placed at ~5 mm from the target as shown in Fig.1(b). The neutrons were produced primarily by various (p,n) reactions (as listed in table 1) inside the catcher.

A detector module was created to measure the sub-MeV neutrons by placing a 1-inch square piece of 1 mm thick EJ-426 scintillator [18] over the faceplate of a 2-inch diameter bialkali photocathode (9902B) Photomultiplier tube (PMT) supplied by ET Enterprise[19]. EJ-426 scintillator is made of a homogeneous matrix of fine particles of ^{6}LiF and zinc sulfide phosphor (ZnS: Ag), compactly dispersed in a transparent binder. The scintillator has a 20 ns rise time and 200 ns decay time response. The EJ-232Q scintillator (0.5% quenching, 150 mm diameter and 25 mm thick) detector was deployed to measure the fast neutron part of the spectrum, which was previously calibrated experimentally for MeV neutron energies. Both the EJ-232Q and EJ-426 detectors were placed together inside a housing, with the source to detector distance of 5.6 m and 5.7 m respectively, shielded by 5 cm thick plastic and 5 cm thick Lead blocks (as used in ref. [15]). The PMT for EJ-426 and EJ-232Q were set at +1000 V and -1000 V respectively, in order to obtain measurable neutron signals with high signal-to-noise ratio.

In the EJ-426 scintillator, energetic daughter nuclei are produced via neutron capture reaction with the ^{6}Li nuclei, ${}^6_3\mathrm{Li} + \mathrm{n} \rightarrow {}^3_1\mathrm{H}$ (2.05 MeV) $+{}^4_2\mathrm{He}$ (2.73 MeV), which generate optical photons by scintillating the ZnS phosphor. As shown in Fig. 2(a), the neutron capture reaction has high cross-section for the sub-MeV neutron energies. Since the plastic scintillators, such as EJ-232Q, are sensitive to fast neutrons, using EJ-426 alongside EJ-232Q, therefore, enables extending the range of our spectral measurement down to keV energies. The amount of light generated from different neutron energies in the EJ-426 scintillator was calculated using Monte-Carlo simulations, carried out considering the statistical nature of neutron capture reaction and the energy loss of daughter nuclei inside the scintillator. A series of FLUKA [20] simulations were performed by irradiating 1μm-thick scintil-

Reaction	$E_{th}(MeV)$	C/S (b)
$^7Li(p,n)^7Be$	1.88	0.27
$^7Li(p,n)^7Be^*$	2.38	0.4
$^7Li(p,n^3He)^7He$	3.68	0.24
$^7Li(p,n)^7Be^{**}$	7.06	0.08
$^7Li(p,np)^6Li$	8.29	0.04
$^7Li+p\longrightarrow n+p+d$	9.98	0.04
$^7Li+p\longrightarrow n+2d$	9.98	0.04
$^7Li+p\longrightarrow n+p+t$	9.98	0.04
$^7Li(p,nd)^5Li$	12.23	0.033

TABLE I. The reaction channels in ^{7}Li(p,n)^{7}Be. E_{th} and C/S are representing the energy threshold and cross-section respectively. (*donates an excited level).

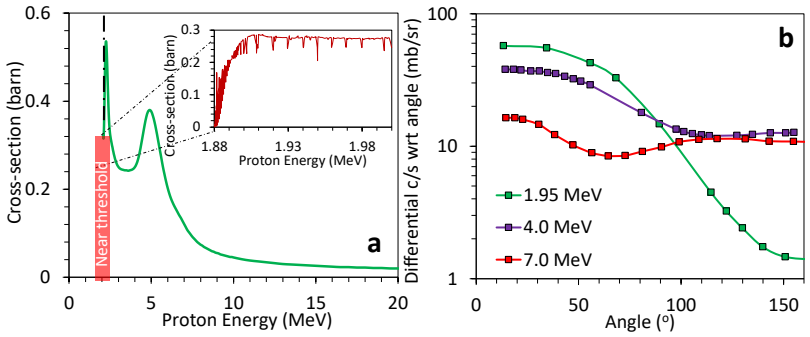

FIG. 3. **(a)** The total cross-section for (p,n) reaction in ^{7}Li, with **(b)** showing the angular distribution of neutrons for different input proton energies. Figure adopted from data reported by ENDF [16].

lating medium for different input neutron energies. The total number of alpha particles produced for each neutron energy is plotted in Fig.2(a). Using the stopping range of alpha particles in the scintillating medium, obtained by employing SRIM[21] code, the light outputs by the alpha particles of different energies were calculated in units of equivalent-electron energy (eVee) using the Chou's semi-empirical formulae [22] as shown in Fig.2(b). Finally, the weighted average scintillation light output $L_n(E_n)$ for a given incident neutron energy E_n was obtained by integrating the light output from all the ions produced by the neutron [15], which is shown in Fig.2(c). As can be seen, the simulated light output as a function of neutron energy, which represents the detector efficiency, follows a similar trend as the reaction cross-section compared to the data reported in *Pino et.al* [23]. As shown our calculation shows a more prominent peak at ∼0.24 MeV, due to the high cross-section of neutron capture resonance peak for that energy region. The detector efficiency was used along with the PMT gain curve (obtained from the manufacture) and transmission curve for the neutrons from source to detector (calculated by a series of FLUKA simulations [15]) were used to deconvolve the ToF data obtained from the EJ-426 detector, in a similar way the data from EJ-232Q is analysed [15]. As will be shown later, the final calibration of the EJ-426 detector for neutron flux was achieved by comparing the fast neutron part of the spectra obtained from both detectors.

Table 1 shows a list of nuclear reactions in ^{7}Li triggered by protons of different energies and their cross-sections, with Fig.3(a) showing the total cross-section for (p,n) reactions in ^{7}Li. The first peak around 600 mB in the cross-section curve for proton energies around 2.25 MeV attributes mainly to the endothermic ^{7}Li(p,n)^{7}Be reaction, which produces a significant amount of keV-MeV neutrons near the reaction threshold - as shown in the insert of Fig.3(a), the cross-section reaches ∼300 mB within 50 keV of the reaction threshold energy of 1.88 MeV[16]. In the near-threshold region, the neutrons are produced by the formation of the ^{7}Be residual, with a narrow energy spread and divergence cone along the proton beam axis, as shown in Fig.3(b). This reaction is one of the of the most frequently studied for accelerator-based compact neutron sources, since it produces mean neutron energy of tens of keV, and requires a small amount of moderation to reach the neutron energy ranges required for many applications, including Boron Neutron Capture Therapy (BNCT)[5].

As the energy of the incident protons is increased, neutron production is augmented by several high yield endothermic reactions, for example, from the first excited state of ^{7}Be at 2.38 MeV, three-body breakup reaction at 3.68 MeV and from the second excited state of ^{7}Be for proton energy above 7.06 MeV. The neutrons produced by these high energy protons carry energy in the MeV range, fairly isotropically as shown in Fig.3(b). The protons accelerated from a laser-driven source typically have a broad spectral bandwidth, as shown in Fig.4(a) obtained from our experiment. In order to optimise the neutron production, a sufficiently thick (∼ 10 mm) block of Li was used. The high energy protons travel deeper in the block, efficiently producing neutrons until their energy drops close to the reaction threshold (1.88 MeV), at which point they produce a substantial number of sub-MeV neutrons with a narrower divergence cone along the proton beam axis.

Fig.4(c) shows a typical raw measurement obtained by the two detectors (EJ-232Q and EJ-426). The gamma flash in the signal was used as a temporal reference to convert the time axis into neutron energy by taking into account the distance from the target to the detector. As can be seen in Fig. 4(c), the signal for sub-MeV neutrons is close to the background level in the EJ-232Q detectors due to their low detection efficiency at these neutron energies. On the other hand, the EJ-426 detector produced a pronounced signal in the sub-MeV range for a reliable spectral measurement. The data from the EJ-426 detector were analysed following the same procedure

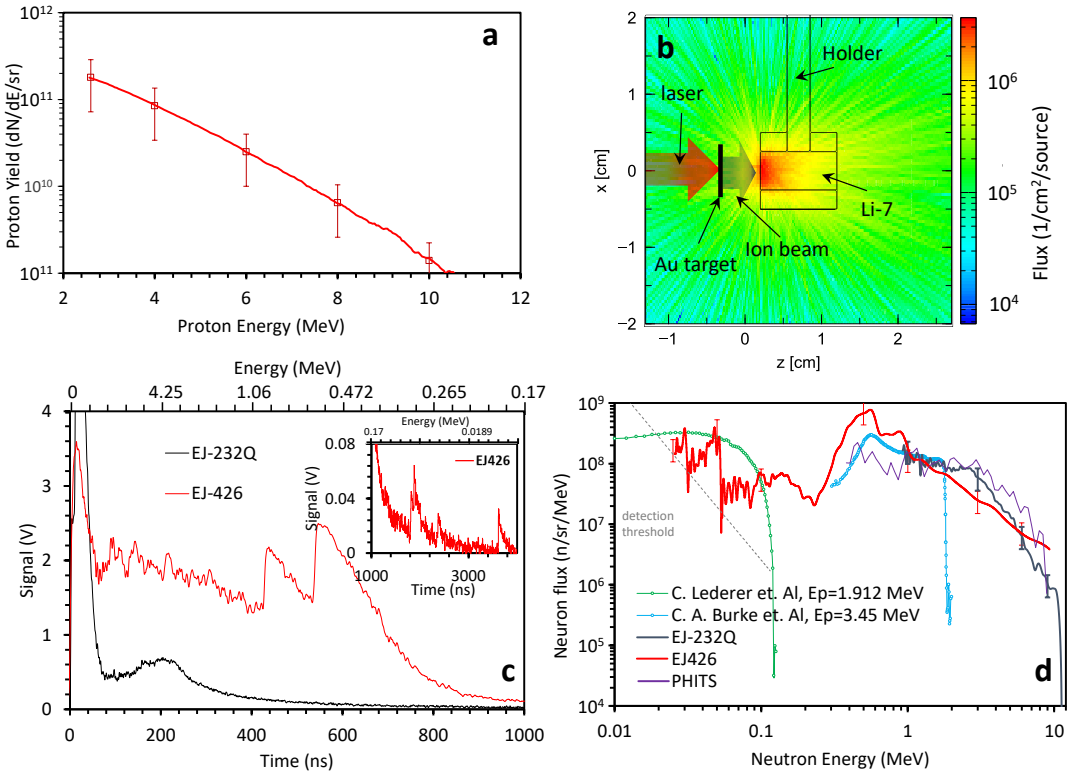

FIG. 4. **(a)** Showing a typical laser-driven TNSA proton spectrum obtained using RCF stacks, **(b)** The 2D map of neutron flux produced by the protons impinging on a Li target, as simulated by the PHITS monte-carlo code. **(c)** Typical raw data obtained from the scintillator detectors. The sharp peak at the early time is caused by the prompt γ. **(d)** Shows the neutron spectra obtained by the EJ-232Q and EJ-426 detectors, where the spectra obtained from the EJ-426 detector is normalised with the EJ-232Q spectrum around MeV energy. The dotted grey line in the figure shows the background signal level for the EJ-426 detector and the data below the threshold were discarded. The purple line shows the neutron spectrum obtained from the PHITS simulation shown in **(b)**. The green and blue lines are the experimental spectrum reported in literature [25, 26] obtained using monoenergetic protons of 1.912 MeV, and 3.45 MeV respectively.

used for the EJ-232Q detector, as described in Mirfayzi et.al [15]. As discussed above, the EJ-426 scintillators are ineffective at measuring the fast neutron part of the spectra, whereas the EJ-232Q are relatively insensitive to sub-MeV neutrons. However, as shown in Fig.4(c), neutrons around MeV energies were adequately detected by both the EJ-426 and the EJ-232Q detectors. The neutron spectrum from the EJ-232Q detector, shown in Fig.4(d), was obtained by using the calibration for neutron flux reported in Ref.[15]. Therefore, cross-calibration of the EJ-426 detector was done by matching the spectra obtained by the EJ-426 and EJ-232Q detectors at neutron energies around MeV, as shown in Fig. 4(d). Interestingly, while neutron flux of $\sim 10^8$ n/MeV/sr was measured for neutron energy above MeV, the data shows a comparable neutron flux of $\sim 10^7$ n/MeV/sr was produced by the near threshold reaction inside the catcher. It is to be noted that the experimental conditions were not varied in the experiment to optimise the neutron yield.

In order to corroborate the experimental data, the neutron source was simulated employing the PHITS-3.08 Monte-Carlo code [24], while using the measured spectrum of the incident protons on the Li catcher (shown in Fig. 4(a)). As shown in Fig. 4(d), a good agreement is found between the simulated spectrum and the experimental data for the first neutron part, showing an isotropic emission from the catcher, as shown in Fig. 4(b). The simulation could not reproduce the sub-MeV part of the measured spectra due to the limitation of the code in simulating the near-threshold reaction. However, the experimental data is over-plotted with the typical neutron spectra reported in the literature using monoenergetic pencil beams of energies as labeled in Fig. 4(d), from conventional accelerators [25, 26]. Although the neutron spectrum from a poly-energetic, divergent source of protons is expected to be different from that produced by an accelerator beam, overall spectral profiles are in broad agreement with each other. As the sub-MeV neutrons are directly produced at the catcher, their pulse duration is determined by the duration of the impinging pro-

ton pulse. Since the burst duration of the laser-driven protons at its source is of a few ps, for our experimental setup (Li catcher at 5 mm from the source, bombarded by protons of 1.88-10 MeV), one can calculate the neutron pulse duration to be no more than 100 ps. In addition to its ultra-short duration, the sub-MeV neutrons measured in the experiment along the proton beam axis were produced with a strong beamed feature, as suggested by the differential cross-section of the near-threshold reaction shown in Fig. 3(b), which is also favourable for further transport and moderation.

While these proof-of-principle results are encouraging, there is significant scope for optimising the laser-driven sub-MeV neutron source. In the current experiment, the near threshold reaction from high energy protons took place deep inside the target, while producing a large number of undesired fast neutrons and broadening the duration of the sub-MeV bursts. The input proton spectrum can be tuned to lower temperature by reducing the laser intensity on the foil target, either by increasing the focal spot size [27] or the laser pulse duration [28]. For given laser energy, reducing the proton beam temperature by decreasing laser intensity also leads to an enhancement in the proton at the lower temperature, which will augment the sub-MeV neutron yield. In conclusion, we have reported bright, ultrashort source of epithermal neutrons produced via ^{7}Li(p,n)^{7}Be reaction at near-threshold employing laser-driven protons on a proof-of-principle basis. The neutron spectrum from the source was measured spanning from tens of keV to tens of MeV by employing a ^{6}Li based scintillator detector together with a fast plastic neutron scintillator. A significant flux of $\sim 10^{7}$ n/sr/MeV/pulse in the sub-MeV region was produced by the laser-driven protons, with intrinsically hundreds of ps burst duration and beamed emission profile. Such compact and intense source of epithermal neutrons would not only be indispensable for cutting-edge applications in industry, security and healthcare, but also for moderating efficiently down to an ultra-compact, bright source of sub-keV and sub-eV neutrons for scientific applications. Finally, the current progress in table-top laser systems, such as diode pumped lasers (DiPOLE) [29] and High-repetition-rate Advanced Petawatt Laser System (HAPLS) [30] will enable the development of stable systems delivering tens to hundreds of Joules at 10 Hz to 100 Hz facilitates leading to the production of compact high repetition rate Petawatt-class neutron sources in coming years.

The authors acknowledge funding from EPSRC [EP/J002550/1-Career Acceleration Fellowship held by S. K., EP/K022415/1], STFC grant ST/P000134/1, EP/R006202/1, ST/P000177/1 and A-STEP (AS2721002c) commissioned by JST. Authors also acknowledge the support of ESG, mechanical and target fabrication staffs of the Central Laser Facility, STFC, UK.

* s.kar@qub.ac.uk

[1] K.W.D. Ledingham, P. McKenna, R.P. Singhal *Sci.* **300**, 1107 (2003).
[2] S. Nakai *J. of Phys.*, **112**, 042070 (2008).
[3] S.R. Mirfayzi, A. Alejo, H. Ahmad, L. Wilson, S. Ansell, *et al. J. Inst.* **11**, C10008 (2016).
[4] B.D. Sowerby, J.R. Tickner, *Nucl.Inst. Met.* **580**, 799 (2007).
[5] R.F. Barth, H. Soloway, R.G. Fairchild, R.M. Brugger, *J. Cancer* **70(12)**, 2995 (1992).
[6] S.R. Mirfayzi, A. Alejo, H. Ahmad, D. Raspino, S. Ansell, et.al. *et al.*, *App. Phys. Let.*, **111(4)**, 044101 (2006).
[7] S. Kar, A. Green, H. Ahmed, A. Alejo, *et al.*. *New J. Phys* **18**, 053002 (2016).
[8] M. Bee *et al.*, *Quasielastic neutron scattering*, (1988).
[9] S. Imberti, C. Andreani, V. Garbui, G. Gorini, *et al.*, *Nucl. Instrum. Meth. A* **552** 463 (2005).
[10] E.P. Cippo, G Gorini, M Tardocchi, C Andreani, A Pietropaolo, R Senesi, N J Rhodes and E M Schoonveld, *Meas. Sci. Technol.* **19** 047001 (2008).
[11] J. Fuchs, P. Antici, E. dHumires, E. Lefebvre, M. Borghesi *et al.*, *Nat. Phys.*, **2**, 48 (2006).
[12] F. Kappeler, F. Thielemann, and M. Wiescher, *Annu. Rev. Nucl. Part. Sci*, **48**, 175 (1998).
[13] E. M. Burbidge GR Burbidge, WA Fowler, F Hoyle, *Rev. Mod. Phys.*, **29**, 547 (1957).
[14] C. Brenner, S.R Mirfayzi, D.R Rusby, C Armstrong, A Alejo *et al. Plasm. Phys. Cont. fus.* **58.1**, 014039 (2015).
[15] S.R. Mirfayzi, S. Kar, A. Ahmed, H. Krygier, *et al. Rev. Sci. Inst.* **86**, 073308 (2015).
[16] H. Liskien and A. Paulsen, *Atomic data nuc. data tab.*, **15(1)**, 57-84 (1975).
[17] C. Danson,P.A. Brummitt, R.J. Clarke, J.L. Collier, *et al. Nucl. Fus.* **44**, S239 (2004).
[18] EJ-426J data sheet, https://eljentechnology.com
[19] ET Enterprises, http://et-enterprises.com/
[20] A. Ferrari et al. FLUKA: A multi-particle transport code (2005).
[21] J.F. Ziegler, SRIM. Cadence Design Systems, 2008.
[22] G. ORielly N.R. Kolb, and R.E. Pywell, *Nucl. Instrum. Meth. A* **368**, 745 (1996).
[23] F. Pino L. Stevanato, D. Cester, G. Nebbia, L. Sajo-Bohus and G. Viesti *J. Inst.* **10.8**, T08005 (2015).
[24] T. Sato, Y Iwamoto, S Hashimoto, T Ogawa *et al. J. Nucl. Sci. Technol*, **55**, 648 (2018).
[25] C. Lederer,F Kppeler, M Mosconi, R Nolte, M Heil *et al. Phy. Rev. C* , **85.5**, 055809 (2012).
[26] C. A. Burke, MT Lunnon, HW Lefevre *Phys. Rev. C* , **10**, 1299 (1974).
[27] C. Brenner, P McKenna, D Neely *Plasm. Phys. Cont. fus.*, **56**, 084003 (2014).
[28] P. McKenna, F. Lindau , O. Lundh , D. Neely , A. Persson , and Claes-Gran Wahlstrm *Rev. Sci. Inst.*, **73**, 4176 (2002).
[29] S. Banerjee, K Ertel, PD Mason, PJ Phillips *et al. Opt. Exp.*, **23(15)**, 19542 (2015).
[30] T. Butcher, PD Mason, S Banerjee, J Pilar *et al. Adv. Sol. Stat. Las.*, **50** (2014).